

# ENVIRONMENTAL STRENGTH EVALUATION OF WELDED STEEL JOINT IN SEA WATER

## PART II : CORROSION FATIGUE CRACK GROWTH BEHAVIOUR

Se-Hi Chung\* and Eui-Gyun Na\*\*

(Received August 14, 1989)

Corrosion fatigue crack growth behaviours were experimentally evaluated for the parent metal, as-welded and PWHT specimens of SM53B steel. Multi-pass welding was done by a submerged arc welder. Metallographic observations along the weld fusion boundary were made to investigate the variation of microstructures through the thickness direction. PWHT was carried out at 650°C with holding time of 1/4hr and 40hr. The corrosion fatigue test was conducted in 3.5% NaCl solution with the frequency of 3Hz. In all cases, crack growth in corrosive environment was faster than that of in air. Besides, at the low  $\Delta K$  region, crack growth was greatly influenced by corrosive environment and the heat treatment condition.

**Key Words :** Post Weld Heat Treatment(PWHT), Heat Affected Zone(HAZ), Residual Stress, Microstructures, Stress Intensity Factor Range, Corrosion Fatigue, Corrosive Environment, Electrochemical Reaction

### 1. INTRODUCTION

It is necessary to evaluate the fatigue behaviours, environmental strength and fracture toughness at weld HAZ for the safe design of the weldments. The HAZ has very complicated and discontinuous structures formed from different thermal cycles and involves the triaxial residual stress (Phillip, 1983 ; Frost et al. 1981). The triaxial residual stress at HAZ results in significant decrease of fracture toughness and acts to promote the fatigue crack growth, just like high stress ratio (Gurney, 1980).

Therefore, post weld heat treatment(PWHT) is conducted to remove the residual stress at HAZ above 600°C. According to the study on PWHT specimens (Lim & Chung, 1988), PWHT embrittlement was dependent upon PWHT conditions through the COD fracture toughness test.

Most fractures of the weldments originate from the weld HAZ under the fatigue load and aggressive conditions mechanically and environmentally in practical engineering fields. However, the fatigue and corrosion fatigue data of PWHT specimens in corrosive environment are scarce.

The purpose of this study is to evaluate the effects of PWHT on the fatigue and corrosion fatigue crack growth behaviors.

### 2. EXPERIMENTAL PROCEDURES

#### 2.1 Welding And Specimens

The material used in this study was SM53B steel with Nb element. Chemical compositions and mechanical properties

are given in Table 1. Steel plate of 30mm in thickness was cut to 100×200(mm) and 45° shaped groove was made perpendicular to the rolling direction and submerged arc welding was performed with seven passes. The welding condition per each pass was given in Table 2. Multipass arc welding produce a wide variety of structures in the HAZ along the fusion boundary through thickness due to the thermal histories (Suzuki, et al, 1976).

Figure 1 shows microstructures at the toe HAZ and midsection regions to the thickness direction indicated by Fig.2. The transformed toe HAZ can be divided into three regions as shown in Fig.1(a), where coarse grained, medium and fine grained structures are denoted as A, B, C. In the meanwhile, various HAZ structures are observed in the HAZ region through the plate thickness except the toe HAZ, which are shown in Fig.1(b). HAZ structure of G region was transformed by the first bead and it changed to tempered martensite by the subsequent weld bead. HAZ structures adjacent to the weld fusion boundary of the second bead was similar to that of the first one. However, the microstructures of D and E

**Table 1** Chemical compositions and mechanical properties  
(a) Chemical compositions, (Wt %)

| C    | Si   | Mn   | P    | S     | Nb    | SoAl  |
|------|------|------|------|-------|-------|-------|
| 0.16 | 0.44 | 1.35 | 0.02 | 0.003 | 0.027 | 0.047 |

(b) Mechanical properties

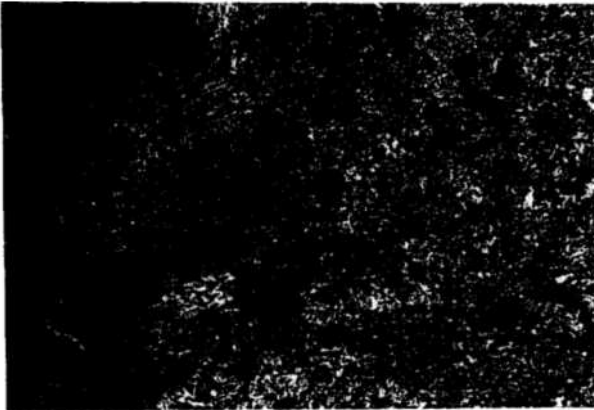
| Yield Strength (MPa) | Tensile Strength (MPa) | Elongation (%) |
|----------------------|------------------------|----------------|
| 372                  | 530                    | 26.7           |

**Table 2** Welding condition

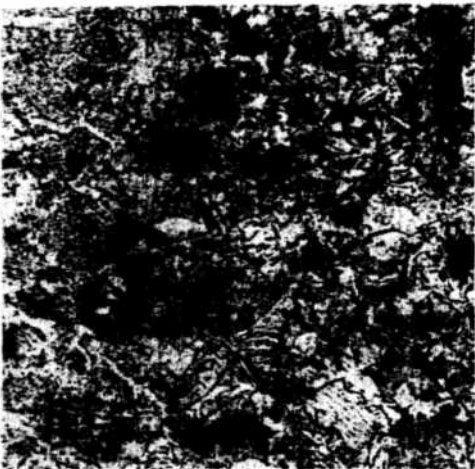
| Heat input (KJ/cm) | Preheat temp.(°C) | Current (A) | Voltage (V) | Welding Speed (cm/min) | Wire dia (mm) |
|--------------------|-------------------|-------------|-------------|------------------------|---------------|
| 30                 | 200               | 650         | 35          | 49                     | 4.0           |

\*Department of Precision Mechanical Engineering, Chonbuk National University, Chonju 560~765, Korea

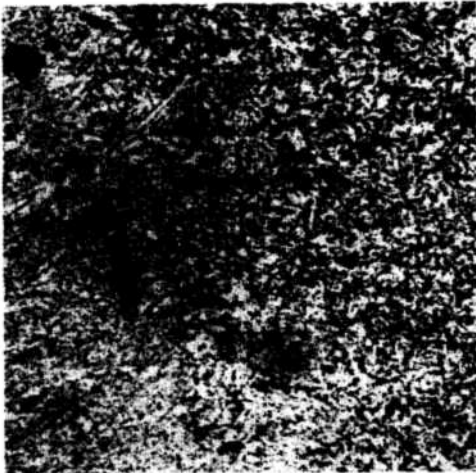
\*\*Department of Marine Mechanical Engineering, Kun San National Fisheries Junior College, Kun San 573-400, Korea



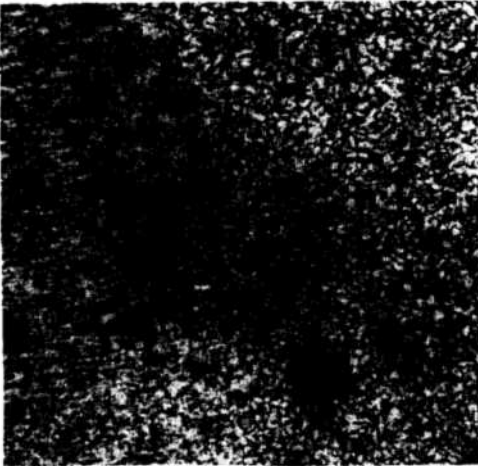
(a)



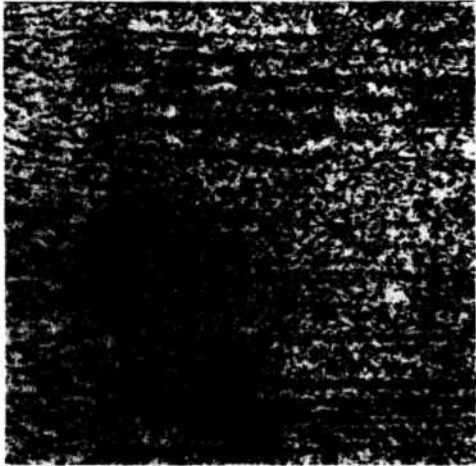
G region



F region



E region



D region

(b)

Fig. 1 Microstructures in toe HAZ and various HAZs in midsection for the weldment

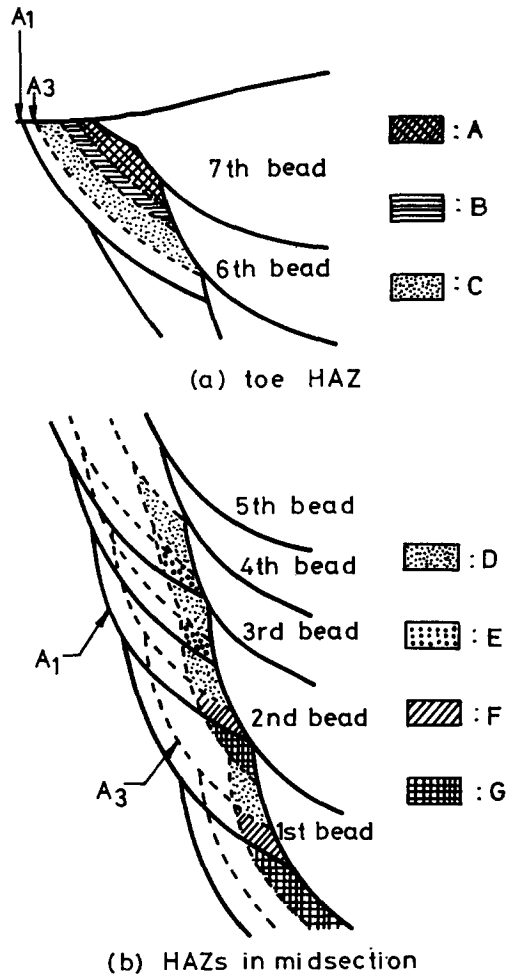


Fig. 2 Schematic illustration of HAZs associated with welding thermal cycles

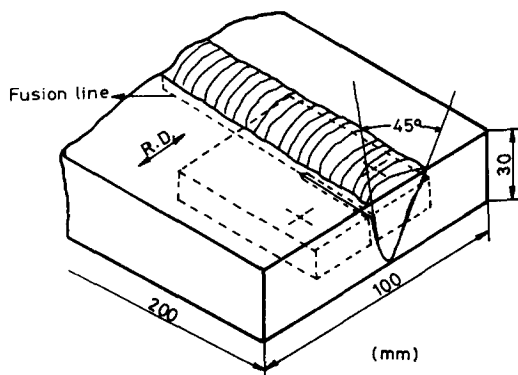


Fig. 3 Weld configuration and extraction of specimen

regions were different from that of *F* region. That is, since the distance between beads become narrower and HAZ structures are subjected to heat treatment by the subsequent beads consequently, the microstructures of *D* and *E* regions are changed to the finer structures due to the recrystallization. Accordingly, those regions consist of the fine ferrite and pearlite structures mainly.

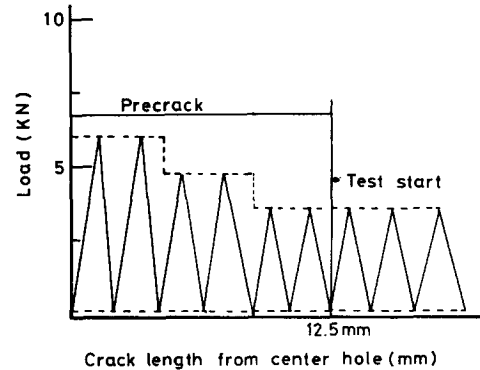


Fig. 4 Load spectrum for precrack making

Table 3 Hardness Value ( $H_{nv}$ ) in HAZS

| As-welded | PWHT 1/4hr   |            | PWHT 40hr    |            |
|-----------|--------------|------------|--------------|------------|
|           | 1/2 CT spec. | Weld block | 1/2 CT spec. | Weld block |
| 294.3     | 254.4        | 258.1      | 225.1        | 240        |

Figure 3 shows the weld configuration along with the position of half sized compact type(CT:B=12.5mm) specimens which are extracted from the second bead to sixth one. The machined crack was made to 14.75mm with the metal saw to the welding direction and then extended by 2mm using the cut-off wheel of 0.14mm thickness. All specimens were precracked approximately to 2mm. Precracking was made in three load steps as shown in Fig.4. The reduction of  $P_{max}$  between load steps was less than 20% according to ASTM standard E647(ASTM standard E647, 1987).

Heat treatment was performed on the half sized CT specimens and weld blocks as following conditions; heating rate of 220°C/hr, heating temperature of 650°C, holding time of 1/4hr and 40/hr, cooling in furnace. In the meanwhile, the microhardness test was made to find out the change of the mechanical property by PWHT. Table 3 shows the results.

## 2.2 Fatigue and Corrosion Fatigue Tests

Fatigue test was performed using a closed loop electrohydraulic testing machine under the load control. Constant amplitude test was conducted with stress ratio,  $R = P_{min}/P_{max}$  of approximately zero(0.05) using a sine wave with the frequency of 3Hz. Crack growth was monitored by the traveling microscope(x30). Corrosion fatigue test was carried out in 3.5% NaCl solution. During corrosion fatigue test, 3.5%NaCl solution was circulated through the acryl cell at a flow rate about 200ml/min. In the meanwhile, when crack propagation path was deviated from the line by above 1.5mm, that data were discarded in this study.

## 3. RESULTS AND DISCUSSION

### 3.1 Crack Growth Behaviours in Air

Figure 5 represents the relationship between crack growth rate and stress intensity factor range for the parent metal and as-welded specimen in air. At the constant  $\Delta K$  value, crack growth rate of the as-welded specimen in air was slower than

that of the parent. These results are in good agreement with the past results (Kapadia, 1978, Na, 1987). Decrease of crack growth for the as-welded specimen is attributed to the compressive residual stress produced by welding and the singularities in welded region such as the discontinuous microstructures, irregularities of mechanical properties and microdefects in HAZ.

Figure 6 is the semilogarithmic plots of crack growth rate and stress intensity factor range for PWHT specimens with the as-welded data. Regardless of the half sized CT specimens and weld blocks subjected to 1/4hr and 40hr holding time, crack growth rate of PWHT specimens is faster than that of

as-welded specimen. It is considered that increased crack growth of PWHT specimens is due to the removed residual stress and uniformization of the microstructures at HAZ by PWHT. Besides, crack growth behaviors between the half sized CT specimens and weld blocks show little difference. This means that fatigue behaviors are independent upon the size of specimens which are given to PWHT. Crack growth rate of PWHT specimens with 40hr holding time is somewhat faster than that of ones with 1/4hr over the all  $\Delta K$  range. These results can be explained as following fact. As can be certified in Table 3, the amount of softening at HAZ with 40hr holding time is greater than that of 1/4hr so that the plastic deformation at the crack tip is easy in the course of crack growth.

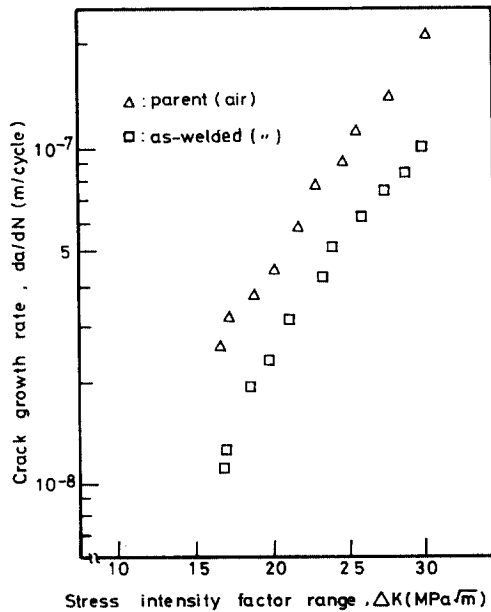


Fig. 5 Crack growth rate versus stress intensity factor range for parent metal and as-welded in air

### 3.2 Crack Growth Behaviour in Corrosive Environment

As reported in previous work (Chung, et, all, 1989), crack growth in corrosive environment was slower than that in air because of the crack branch, crack closure and secondary cracks which are formed at HAZ. In this study, the evaluation of crack growth behaviours was made on the relationship between  $\Delta K$  and the  $da/dN$  obtained in corrosive environment by comparing with the data in air.

Figure 7 shows the corrosion fatigue crack growth behaviour for the parent and as-welded specimen including the air data. Regardless of the specimens, crack growth rate in 3.5% NaCl solution increased compared with those in air. This means that corrosion fatigue crack growth behaviours are dependent upon the loading method and experimental conditions.

Figure 8 represents the relationship between  $\Delta K$  and  $da/dN$  for PWHT specimens in 3.5% NaCl solution with the air data. Crack growth rate in corrosive environment is faster than that in air over the all  $\Delta K$  range, unlike the results obtained in previous study (Chung, et, al, 1989). Besides, at the

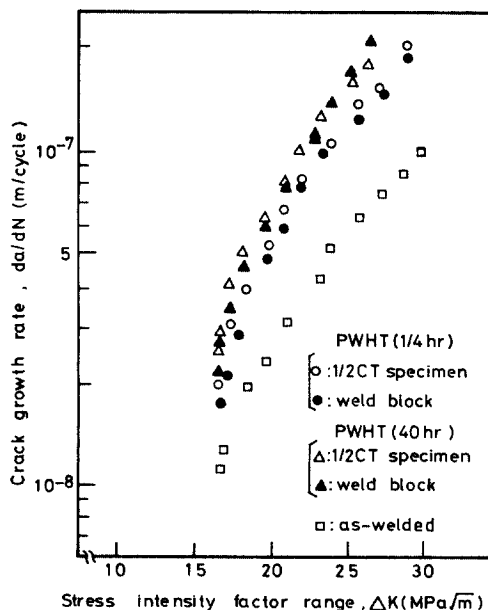


Fig. 6 Crack growth rate versus stress intensity factor range for PWHT specimens and as-welded in air

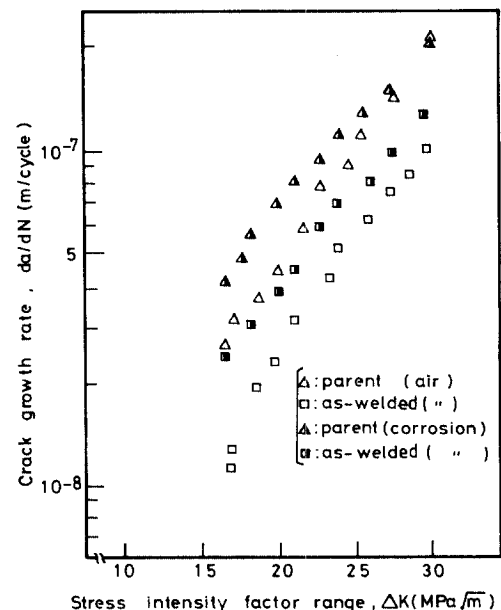


Fig. 7 Crack growth rate versus stress intensity factor range for parent metal and as-welded in 3.5% NaCl solution, including the air data

low  $\Delta K$  region which shows the slow crack growth rate, fatigue crack growth in 3.5% NaCl solution was greatly influenced by corrosive environment. However, as value of  $\Delta K$  increases, crack growth rates measured in NaCl solution approached the data obtained in air. These results are similar to the past study (Lee, et. al). This means that as the crack grows, the net section area of the specimens decreases. So, at the higher  $\Delta K$  region, the mechanical factors rather than environmental ones give the predominant influence to crack growth. In this experiment, the accelerated crack growth in corrosive environment is based on the electrochemical theory of the crevice corrosion (Son, 1980).

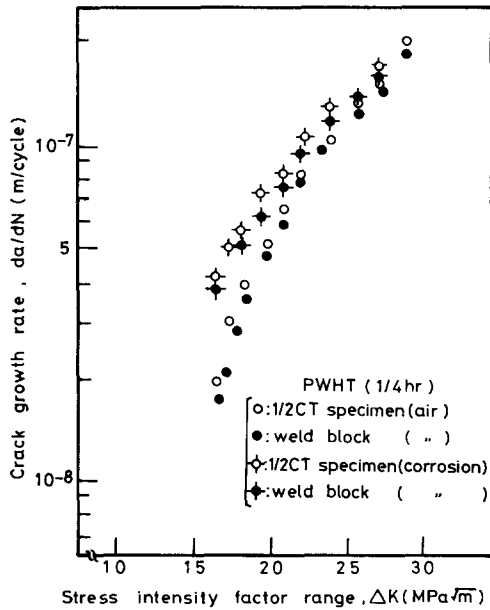


Fig. 8 Corrosion fatigue crack growth behaviour for 1/4hr PWHT specimens with the air data

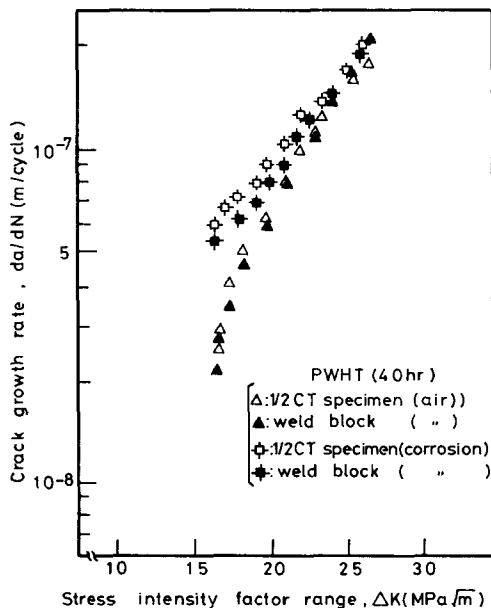
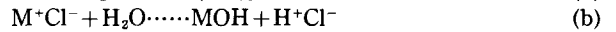


Fig. 9 Corrosion fatigue crack growth behaviour for 40hr PWHT specimens with the air data

That is;



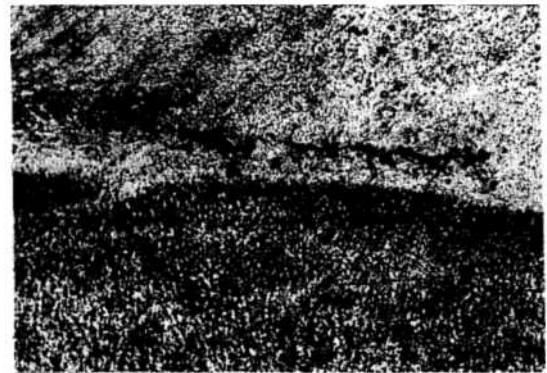
Hydrogen gas which is produced by hydrolysis (a) is absorbed at the plastic zone at the crack tip and then hydrogen embrittlement at the crack tip occurs. The metals at the crack side and tip are dissolved into corrosive environment. In this experiment, electrochemical reaction mentioned above between the crack and corrosive environment occurs enough, whereas not at high cycle. So, these two mechanisms such as hydrogen embrittlement mechanism and dissolution mechanism cause to increase the crack growth in corrosive environment.

Figure 9 represents the corrosion fatigue crack growth behaviours for 40hr PWHT specimens with the air data. Crack growth rate in corrosive environment was increased compared with that in air. Besides, at low  $\Delta K$  region, corrosion fatigue crack growth for this condition is faster than that of 1/4hr holding time specimen. This means that crack growth in 3.5% NaCl solution is dependent upon the holding time during PWHT.

### 3.3 Fractography

The fracture surfaces and microstructures at HAZ were examined to determine the fracture mechanisms.

Figure 10 shows the crack propagation path on the surface at HAZ. The singularities at HAZ such as discontinuous



(a)



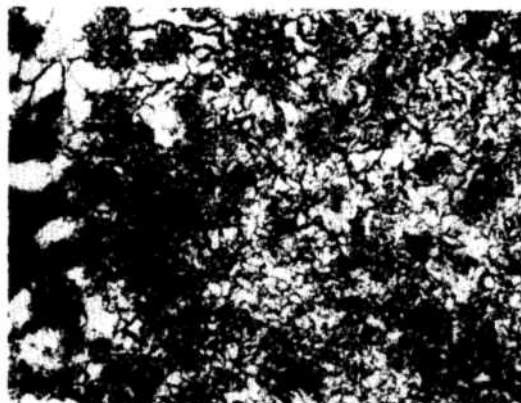
(b)

Fig. 10 Crack propagation path on specimen surface at HAZ



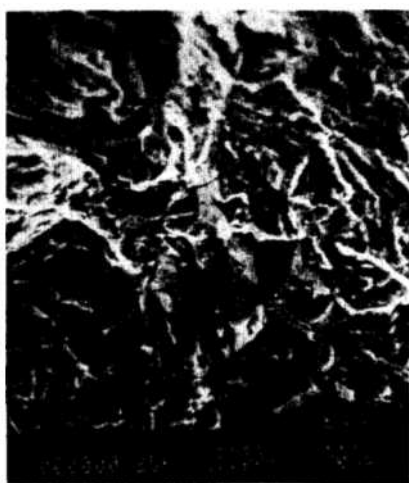
(a)

PWHT, 1/4hr

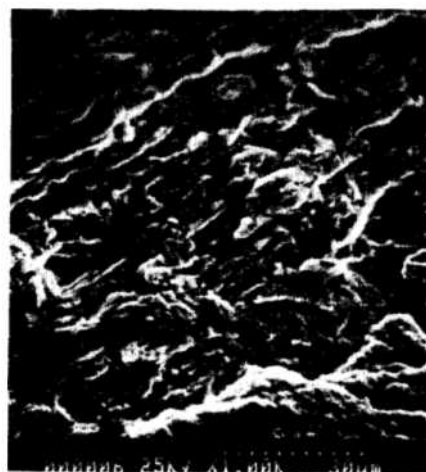


(b)

PWHT, 40hr



(c)

PWHT, 1/4hr ( $\Delta K \approx 20\text{MPa}\sqrt{\text{m}}$ )

(d)

PWHT, 40hr ( $\Delta K \approx 20\text{MPa}\sqrt{\text{m}}$ )

**Fig. 11** Change of microstructures and fracture surfaces at HAZ subjected to PWHT of 1/4hr and 40hr holding time

microstructures, irregularities of mechanical properties and microdefects make the crack propagation path complex. The zig-zag shape of the crack path was due to the discontinuous microstructures. Especially, the crack branching and crack arresting phenomena at HAZ were produced because of the microdefects which act to blunt the crack.

Figure 11 represents the change of microstructures and fracture surfaces at HAZ which were subjected to PWHT of 1/4hr and 40hr holding time.

Considerable change of microstructures at HAZ can be seen between 1/4hr PWHT specimen and 40hr PWHT one, as shown in Fig.11 (a), (b). Microstructure of PWHT specimen subjected to 40hr was almost uniformized and fine grained structures compared with that of 1/4hr PWHT specimen. Judging from the fact that change of microstructures according to PWHT was believed to give an influence to crack growth rate at HAZ, the fracture surfaces were observed by a scanning electron microscope(SEM), as illustrated Fig.11(c), (d). In the case of 1/4hr PWHT specimen, the surface was composed of intergranular fracture and some amount of transgranular striation, whereas, the surface of 40hr PWHT specimen was mostly transgranular fatigue striation.

## 4. CONCLUSIONS

The effects of PWHT in welded HAZ of SM53B steel on fatigue and corrosion fatigue crack growth behaviors were evaluated. In air, crack growth rate for PWHT specimens increased in comparison to that of the as-welded over the all  $\Delta K$  range. In addition, crack growth behavior is dependent upon the holding time during PWHT. In all cases, crack growth rate in 3.5% NaCl solution was faster than that in air. At the low  $\Delta K$  region, the effect of corrosive environment on crack growth was obvious. However, the corrosion effect decreased with the  $\Delta K$  slowly. Besides, in the case of 1/4hr PWHT specimen, the surface was composed of intergranular fracture and some amount of transgranular striation, whereas, the surface of 40hr PWHT specimen was mostly transgranular fatigue striation.

## ACKNOWLEDGMENTS

This study was supported by the Korea Science and Engi-

neering Foundation (KOSEF). The authors wish to acknowledge the financial aid during the course of this investigation.

## 5. REFERENCE

- ASTM Standard E647, 1987, "Standard Test Method for Constant Load Amplitude Fatigue Crack Growth Rates", 1987 Annual Book of ASTM Standard Vol.03, 01, pp 711~731.
- Chung, S.H., Lim, J.K. and Na, E.G., 1989, "Environmental Strength Evaluation Welded Steel Joint in Sea Water, Part I: Corrosion Fatigue Crack Growth Behaviors for High Cycle", KSME Journal, Vol 3, No.1, pp~5.
- Frost, R.H., Edwards, G.R. and Rheinlander, A.D., 1981, "A Constitutive Equation for the Critical Energy Input during Electroslog Welding", Welding Journal, Jan., pp. 1~6.
- Gurney, T.R., 1980, "Fatigue Welded Structures", Cambridge Univ. Press, 2nd ed.
- Kapadia, B.M., 1978, "Influence Residual Stresses on Fatigue Crack Growth in Electroslog Welds", ASTM STP 648, pp 244~260.
- Lim, J.K. and Chung, S.H., 1988, "Stress Effect on PWHT Embrittlement", Fatigue and Fracture Testing of Welding of Weldments, Edited by H.I. McHenry and J.M. Potter, ASTM STP, to be published.
- Na, E.G., 1987, "Effect of PWHT on Corrosion Fatigue in Weld HAZ of Steels", Doc. Thesis, Jeonbuk National University, Koera.
- Philipp, R.H., 1983, "In Situ Determination of Transformation in the Weld Heat Affected Zone", Welding Journal, Jan., pp 12~18.
- Son, Un Teak, 1980, "Corrosion Theory of Metals".
- Lee, D.N. and Lee, S.K., 1989, "Corrosion Fatigue of SAE 1100 Steel in 3% NaCl Solution", Material Science and Technology, Vol. 5, pp 468~477.
- Suzuki, M., Kameda, J., Takahashi, H. 1976, "Stress Relief and Local Embrittlement of Weld Heat Affected Zone in a Reactor Pressure Vessel Steel" IIW Document No. IX-1002.